

# Simplified, empirical model of wind speed profile under canopy of Istebna spruce stand in mountain valley

Przemysław Sypka<sup>a,\*</sup>, Rafał Starzak<sup>b</sup>

<sup>a</sup> AGH University of Science and Technology, Department of Electronics, al. Mickiewicza 30, 30-059 Kraków, Poland

<sup>b</sup> University of Agriculture in Krakow, Department of Forest Engineering, al. 29 Listopada 46, 31-425 Kraków, Poland

## ARTICLE INFO

### Article history:

Received 22 May 2012

Received in revised form 26 October 2012

Accepted 4 November 2012

### Keywords:

Vertical wind profile  
Forest stem layer  
Forest canopy  
Spruce stand  
Complex topography

## ABSTRACT

The wind speed in a forest is one of the main factors deciding upon the amount of water balance between the atmosphere and the soil. Inside a forest complex, the distribution of vertical wind speed has a characteristic S-shape. This paper presents a simplified, empirical model of such an S-shaped wind profile within a stem layer of an Istebna spruce stand. Measurements of the wind speed were taken at four levels in 9 homogeneous, even-aged stands of different age-class: from a 10-year-old natural seeding to a 121-year-old mature stand. Recorded data unambiguously confirmed the existence of the secondary maximum inside the stem layer. The main aim of this paper was to make all model parameters conditional on biometrics features of tree stand as well as the geographical location of research sites on the slopes in a mountain valley. All parameters describing the simplified, empirical model of S-shaped wind profile within the stem layer strictly depend on the well-known total basal area  $TBA$  [ $m^2 h^{-1}$ ].  $TBA$  is determined by only an average number of trees per hectare and a mean diameter at a breast height, i.e. 130 cm above ground, which are easy to be measured with high accuracy 'from ground'. Presented data analysis shows that the estimated wind speed at the secondary maximum and a mean wind speed within a stem layer are contingent upon a biomass density in the crown layer and its elevation above ground. A biomass density can be equated with the leaf area index (LAI).

The presented simplified, empirical model of the vertical wind speed profile for a spruce stand and its parameterization scheme, which is to be measured in an effortless way, should be easily adaptable to stands composed of other tree species, taking into consideration specific differences between spaces. The necessary improvements of the presented empirical model would be possible after some series of measurements taken within various types of tree stands. A thorough understanding of the biological factors creating the observed S-shaped wind profile ought to considerably expand the knowledge of the forest 'ventilation' process, which determines vaporization from the soil as well as the  $CO_2$  advection.

© 2012 Elsevier B.V. All rights reserved.

## 1. Introduction

The wind velocity in a forest, besides solar energy reaching the surface of the soil and the soil humidity, is the main factor, deciding upon the amount of water evaporating from inter-particle spaces of the soil. In turn, the vaporization from the soil has a basic significance for the components of water exchange balance between the atmosphere, tree stand, and the soil in different forests. The silvicultural practices, which affect the amount of biomass located in various layers of tree stand, may influence the quantity of wind momentum reaching forest floor level. If an energy balance within

a forest community is well known as a physical process, there are still no formulae combining the variability of its components with the biometric features of the tree stand. Due to technical and organizational conditions of field research within tree stands the wind velocity could be measured at a few strictly chosen points at different heights. The development of measurement methods and the automated registering of results create greater opportunities of gathering and processing a huge amount of data. Still, the problem of proper choice of measurement points, especially inside a dense forest complex, essential for identification of theoretical models, and improving the methods of extrapolation of results remain to be solved on a large spatial scale. Although various algorithms have been developed to obtain an accurate spatial distribution from limited measurements (Queck and Bernhofer, 2010; Zhu et al., 2000; Aubinet et al., 2003; Staebler and Fitzjarrald, 2004;

\* Corresponding author. Tel.: +48 12 6172752; fax: +48 12 6332398.  
E-mail address: [sypka@agh.edu.pl](mailto:sypka@agh.edu.pl) (P. Sypka).

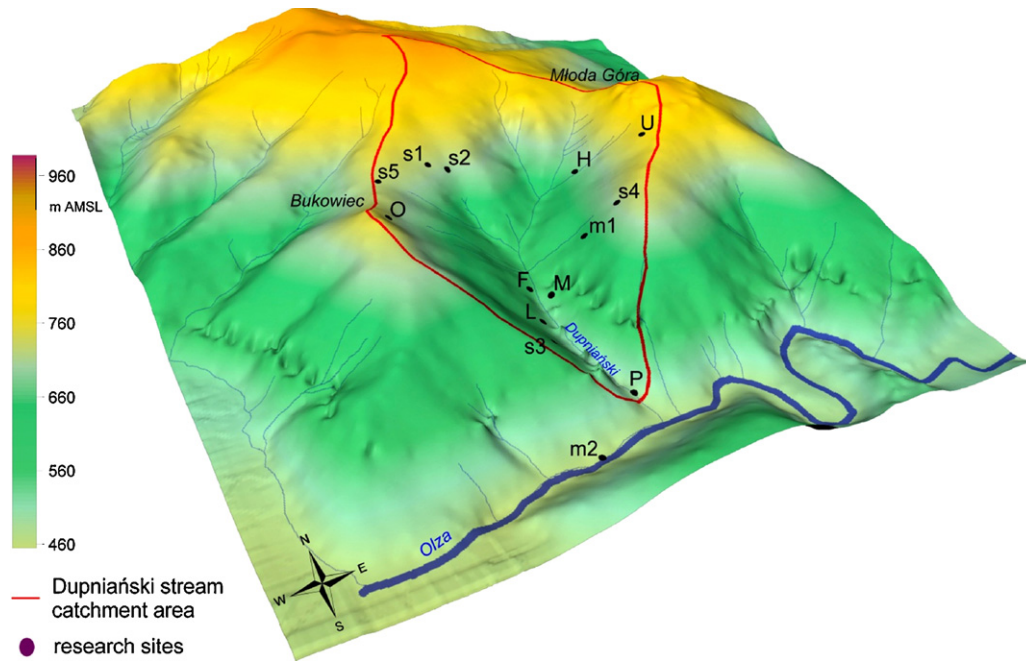


**Fig. 1.** DUPNIAŃSKI STREAM catchment (49°35'N, 18°50'E, total area: 1.68 km<sup>2</sup>, average altitude: 690 m AMSL, valley prominence: 404.4 m, forested by Norway spruce, ecotype the Istebna spruce stand in 95%) and positions of research sites: 14 within homogeneous, even-aged stands of different age-class: from a 10-year-old natural seeding to a 121-year-old mature stand (indicated by capital letters, see also Table 2 and Table 3), 3 in open fields at inter-forest meadows (s5, m1, m2) and a triangle-shaped overflow weir for measuring the total run-off from the catchment (P).

Marcolla et al., 2005; Yi et al., 2005), there is still the lack of an appropriate method to transfer the parameters of the approaches to other sites.

In general, under thermally neutral conditions, a vertical wind speed profile over any rough surface can be described by a well-known logarithmic law:

$$U(h) = \frac{U^*}{\kappa} \cdot \ln \left( \frac{h - h_d}{h_{z_0}} \right) \quad (1)$$

where  $U(h)$  is the wind speed at height  $h$  [m/s];  $U^*$  is the friction velocity [m/s], defined as  $\sqrt{\tau_0/\rho}$ ,  $\tau_0$  is the shear stress at the surface [ $\text{kg m}^{-1} \text{s}^{-2}$ ],  $\rho$  is the air density [ $\text{kg m}^{-3}$ ];  $\kappa$  is the von Karman's constant ( $\approx 0.40$ , dimensionless);  $h$  is the height of measurement from the reference plane [m];  $h_d$  is the zero-plane displacement [m];  $h_{z_0}$  is the roughness length [m] (von Kármán, 1930; Prandtl, 1925). The roughness length is equivalent to the height at which the wind speed theoretically becomes zero. As an approximation, the roughness length is about one-tenth of the height of the surface roughness elements. This classic theory does not work within and under a forest canopy because the vertical wind distribution is not logarithmic (Fons, 1940; Lemon et al., 1970; Bergen, 1971; Landsberg and James, 1971; Oliver, 1971; Shaw, 1977; Meyers and Paw, 1986; Massman, 1987, 1997; Baldocchi and Meyers, 1988; Fischenich, 1996; Massman and Weil, 1999; Lee, 2000; Lalic and Mihailovic, 2002; Turnipseed et al., 2003; Yi et al., 2005; Yi, 2008). In such a situation it is essential to also take under consideration the biometric features of tree stands and not only the heights. Massman (1997) parameterized the canopy horizontal wind speed as exponential function of cumulative leaf drag area per unit planform area. Yi (2008) found that for canopies with uniform vertical distribution of the leaf area index (LAI) the momentum transfer through a canopy can be expressed by the following formula:

$$U(h) = U_H \cdot \exp \left\{ -\frac{1}{2} LAI \left( 1 - \frac{h}{H_c} \right) \right\}, \quad (2)$$

where  $U(h)$  is the wind speed at the height  $h$  within the canopy [m/s];  $U_H$  is the wind speed at the top of the canopy;  $H_c$  is the height of the canopy [m]. These both wind speed profiles are monotonic functions of height,  $h$ , and, therefore, do not produce a secondary maximum within the stem layer.

In a mountainous terrain the shape of the surrounding peaks, passes and valleys is an additional factor that has an influence on observed and measured wind speed. Gauged wind speed can be determined by the orientation of the measuring site (i.e. tilt and azimuth angles, an angle of wind incidence) and by the topography of its closest neighbourhood. The purpose of the present study is to find and test a simple empirical model of the observed S-shaped vertical wind speed profile within the stem layer of the Istebna spruce stand. Additionally, all parameters, used in the model, should be expressed by the biometrical characteristics of the tree stand and locations of the research sites. Such models are essential for forest practice to predict and to describe the effects of silvicultural measures.

## 2. Sites and measurements

The specificity of wind speed measurement inside the tree stand is related to a layered distribution of biomass. The biomass is characterized by changes of quantity and density over time, both in scale of one vegetation cycle as well as over long periods of time.

### 2.1. Research sites

The research sites were located inside the area of the experimental catchment DUPNIAŃSKI STREAM (49°35'N, 18°50'E) in the Silesian Beskid Mountain Range (Poland). The experimental catchment was organized by the Department of Forest Engineering from the University of Agriculture in Krakow. This was a small, mountain catchment (average altitude 690 m AMSL, total area of 1.68 km<sup>2</sup>, maximum length 2.09 km, maximum width 1.47 km, circuit 5.39 km), forested by a Norway spruce stand (*Picea abies* (L)

**Table 1**  
Selected characteristics of the sites and Dupniański stream valley.

Site	Z	Zr	Zrl	H <sub>1</sub>	H <sub>2</sub>	H <sub>3</sub>	H <sub>4</sub>	DY
U	766.5	289.0	206.5 <sup>a</sup>	1.2	–	–	0.4	222–226
S1	717.0	239.5	157.0 <sup>a</sup>	8.4	–	2.2	0.4	203–209
M	550.5	73.0	12.1	19.0	8.2	2.2	0.4	233–238
S2	698.0	220.5	138.0 <sup>a</sup>	16.6	7.4	2.1	0.3	215–222
H	669.7	192.2	109.7 <sup>a</sup>	18.0	7.1	2.2	0.4	227–233
O	723.2	245.7	133.5 <sup>a</sup>	34.7	13.8	2.2	0.4	250–255
L	542.8	65.3	15.1	43.6	25.0	2.2	0.4	245–250
F	556.8	79.3	4.6	42.9	24.9	2.3	0.4	238–245
S4	703.4	225.9	143.4 <sup>a</sup>	38.2	23.3	2.2	0.3	209–215
Valley top	Zvt	881.9						
Valley floor	Zvf	477.5						
Valley prominence	dZv		404.4					

Z, altitude [m]; Zr, relative altitude to the lowest point in the catchment area [m]; Zrl, relative elevation to the local valley floor [m]; H<sub>1</sub>, measurement heights [m] (1 – just above the tree crown, 2 – just under the tree crown, 3 – at the height of about 2.4 m above ground, 4 – at the height of about 0.4 m above ground); DY, days of the investigated year [2004].

<sup>a</sup> Calculated with the reference to the altitude of the recession point of the valley bottom gradient (~560 m AMSL).

Karst., ecotype – the *Istebna spruce*) in 95%. The *Istebna spruce* was distinguished by a very quick growth up to 50 m tall, an extraordinary stem quality, high resistance to different disasters, and productivity up to 1500 m<sup>3</sup>/ha. Spruce stands in this region of the Silesian Beskid Mountains were rated among the best seed forest stands in Europe (Giertych, 1996; Janson, 1996; Pacalaj et al., 2002; Małek and Gawęda, 2005; Liesebach et al., 2010). 18 research sites were deliberately chosen inside the area of the experimental catchment: 14 within homogeneous, even-aged stands of different age-class, 3 in open fields at inter-forest meadows (s5, m1, m2) and a triangle-shaped overflow weir for measuring the total runoff from the catchment (P). The spatial arrangement of all research sites inside the DUPNIAŃSKI STREAM catchment is presented in Fig. 1. All data presented in this paper were gauged at nine research sites: starting from 10-year-old natural seeding (site U), through a thicket (site S1) and maturing stands (sites S2, M and H) to mature forests (sites O, F, S4 and L). The selected characteristics of the research sites and Dupniański Stream Valley are presented in Table 1. The value of a local elevation above the valley floor (Zrl) for high-situated research sites (U, S1, S2, H, and S4) were calculated with reference to the altitude of the recession point of the valley bottom gradient (~560 m AMSL).

The homogeneous, even-aged spruce stands at the research site consisted only of the canopy and the stem layer; there was no forest vegetal cover in vicinity of the selected measurement points. This fulfils the requirements of the spatial averaging scheme (Wilson and Shaw, 1977; Raupach and Shaw, 1982; Finnigan, 1985; Raupach et al., 1986), which maintains the fundamental vertical heterogeneity of the stand but emphasizes its horizontal uniformity. Hence, each layer within the stands at the research sites, i.e. the stems and the crowns, is an endless slab of the specific thickness. In turn, it is possible to assume, in a simplified way, that the distribution of biomass density is uniform in each layer. Even though a biomass distribution is extremely heterogeneous, such an assumption is nearly fulfilled within the stem layer (stems, dry state resulted from self-pruning of dry branches, and air), but inside the canopy (stems, branches, cones, conifer needles, dry state, air) the spatial arrangement of biomass mainly depends on the height (Green et al., 1995) and ought to be understood as a generalization.

The biometric features of the investigated tree stands were measured at circular surfaces around the gauging profiles: area of 3 a in the natural seeding and the thicket (sites U and S1, respectively) and 10 a in other sites. The diameters at the breast height (i.e. 130 cm above ground, DBH) were recorded by using a precision callipers. The heights of trees (H) and the elevation of the crown layer (the height of the stem layer, H<sub>s</sub>) in experimental tree stands were determined in trigonometric way by using the Zeiss Dahlta

O10B tacheometer. The elevation of the crown layer was defined as the height of the lowest green branches. The obtained data were used to calculate the mean diameter at the breast height and the mean tree height by applying Lorey's formula, which is often used in dendrometry (Bruchwald, 1995). Lorey's equation gives a bit higher values than traditional arithmetic average because of a correction to basal area. The height (thickness) of the crown layer was evaluate as the difference between the tree stand mean height and the mean elevation of the crown layer. Thereafter, biomass of leaves (needles) and volume of trunk and small-sized branch wood were estimated for the model mean tree by the method proposed by Suliński (1993, 2007). The empirical equations used in this procedure were identified on data included in the yields tables (Schwappach, 1943) and in the volumetric tables (Czuraj et al., 1966). The total biomass of fresh timber (stem and branches, [tonne/ha]) was approximated by multiplying the model mean tree volume by spruce green wood density (0.75 tonne/m<sup>3</sup> after Suliński (1993, 2007)) and the total number of trees per hectare (N). The total biomass of tree stand was the sum of the total biomass of fresh timber and the total biomass of leaves. The biomass of the canopy was calculated as the difference between the total biomass of tree stand and the total biomass of wood within the stem layer. The calculations of total biomass of stem layer were based on the diameter of trunk at the stem mid-height and the mean trunk taperness. The results (standardized for 1 ha) are shown in Table 2. The detailed equations used to estimate the biometric features of tree stand are included in Appendix.

The total basal area TBA [m<sup>2</sup> ha<sup>-1</sup>] was calculated as a multiplication of the number of trees per hectare (N) and the area of vertical projection of a stem profile – approximated circle with the diameter equal to mean diameter at the breast height (DBH [cm]):

$$TBA = \frac{N \cdot \pi \cdot (DBH/100)^2}{4} \quad (3)$$

Biomass density in both a stem layer and crown layer was calculated as a ratio of an estimated biomass in a given layer to the height of this layer  $R_i = M_i/H_i$  [tonne of fresh mass per 1 ha per 1 m].

## 2.2. Measurements

Extensive research on the water exchange balance between the atmosphere, tree stand, and the soil of *Istebna spruce* stands was carried out in 2004 during the summer period (from 22-07-2004 to 12-09-2004). All measurements were gauged at 4 levels (Table 1): just above the treetops (H<sub>1</sub>), just under the tree canopy (H<sub>2</sub>), at the heights of about 2.2 m and (H<sub>3</sub>) and 0.40 m (H<sub>4</sub>) above the ground. The wind speed, solar radiation intensity, air temperature and humidity were measured at every level. Air pressure was

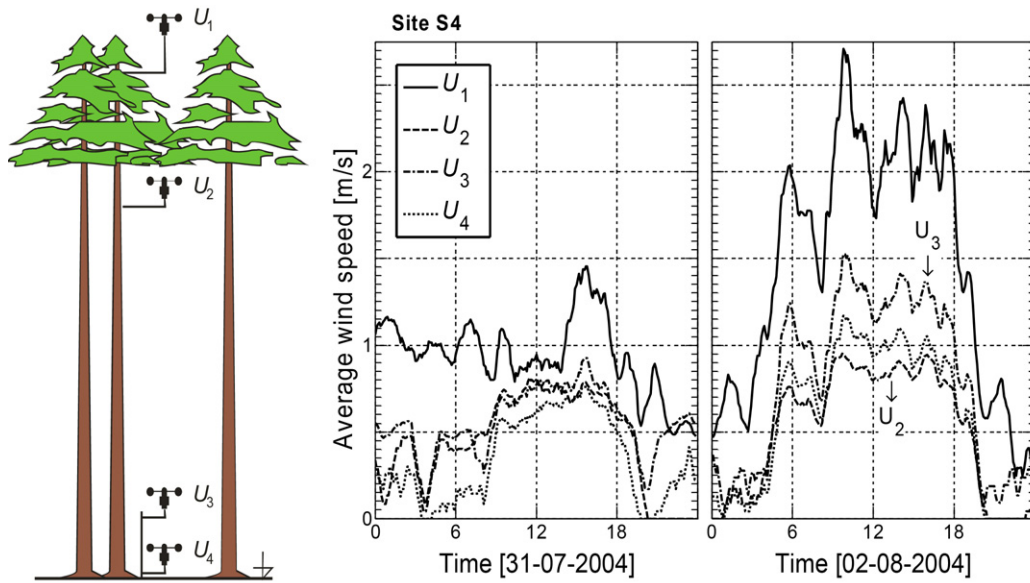


**Fig. 2.** Scheme of gauging section (left) and examples of mean wind velocity waveforms measured in investigated sites (right). Three-cup anemometers were used to gauge wind speeds at 4 levels: just above the treetops ( $U_1$ ), just under the canopy ( $U_2$ ), at the heights of about 2.2 m ( $U_3$ ) and 0.4 m ( $U_4$ ) above the ground. Recorded data show characteristic changeability: for light wind above the crown layer wind velocity plots in the stem layer are very similar (see plots on the 31st of July 2004), but when the wind speed over treetops ( $U_1$ ) is sufficiently high ( $U_1 > 1.5$  m/s) then the wind velocity waveforms in the stem layer become disjointed (see plots on the 2nd of August 2004).

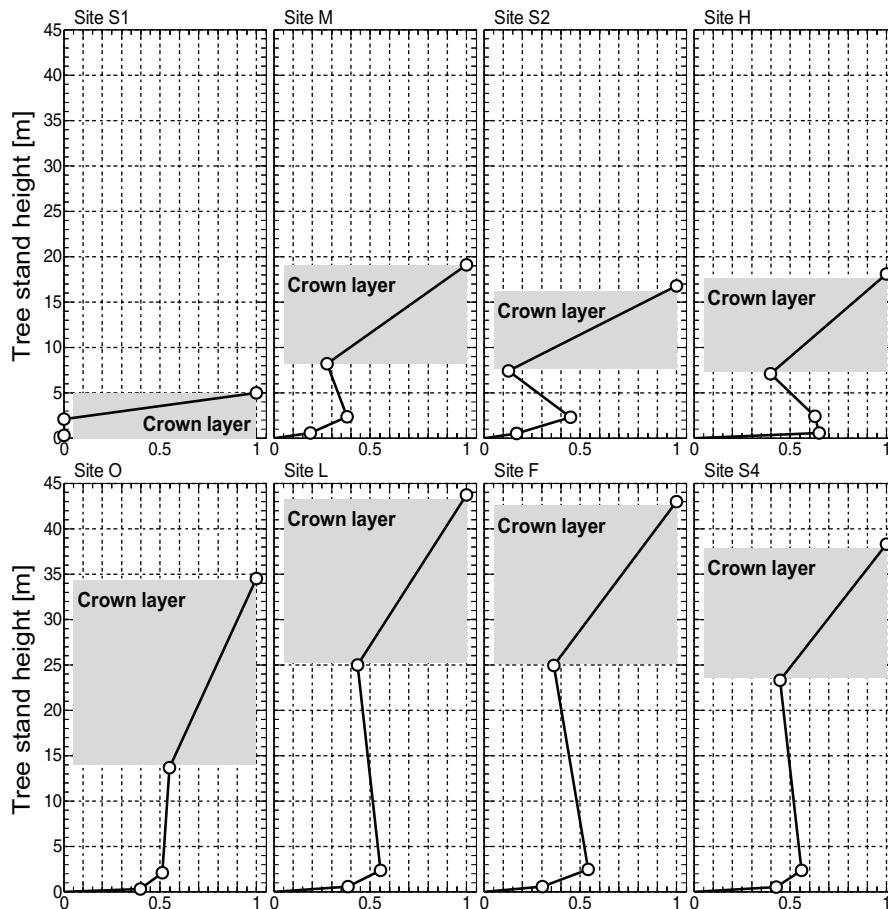


**Fig. 3.** Gauged wind speed profiles normalized with the wind speed over tree tops ( $U_1$ ) in investigated stands: a thicket (site S1, age: 16, no stem layer), maturing stands (sites S2, M and H, age: 26–41) and old forests (sites O, L, F and S4, age: 96–121). The characteristic S-shaped pattern can be distinguished in all research sites except for the site O. It may result from the location of this research site just near border of the catchment area (see Fig. 1), which followed the Ridge of Bukowiec Mountain (750 m AMSL). In such a case this site could have been over-exposed to a wind force considerably stronger than to other sites (not only from the 'heart' of Dupniański stream valley).



**Table 2**  
Empirical data and calculated biometric features of the stands at the investigated sites (Suliński, 1993, 1997).

Site	A	N	D	TBA	H	Hs	Hc	Ms	Mc	Rs	Rc
U	10	26,800	1.4	4.1	0.8	–	0.8	–	37.0	–	46.25
S1	16	13,758	3.6	14.0	5.0	–	5.0	–	89.9	–	17.98
M	26	2038	16.9	45.7	18.6	8.4	10.2	239.9	205.2	24.43	23.52
S2	29	2070	14.7	35.1	16.2	7.6	8.6	174.2	143.2	18.84	20.26
H	41	2134	17.1	49.0	17.6	7.3	10.3	201.1	258.9	27.55	25.14
O	96	318	41.7	43.4	34.3	14.0	20.3	257.8	317.9	22.71	12.70
L	96	287	47.8	51.5	43.2	25.2	18.0	254.9	537.6	21.33	14.16
F	116	255	50.1	50.3	42.5	25.1	17.4	235.3	511.6	20.38	13.52
S4	121	330	45.5	53.7	37.8	23.5	14.3	250.2	495.1	21.07	17.50

A, age [year]; N, number of trees per 1 ha; D, average diameter at the breast height (DBH) [cm]; TBA, the total basal area [ $\text{m}^2 \text{ha}^{-1}$ ]; H, average stand height [m]; Hs, the height of the layer of stems [m]; Hc, the height of the layer of tree crowns [m]; Ms, mass of the layer of stems [t of fresh mass  $\text{ha}^{-1}$ ]; Mc, mass of the layer of the tree crowns [t of fresh mass  $\text{ha}^{-1}$ ]; Rs, biomass density of the layer of stems [ $\text{t ha}^{-1} \text{m}^{-1}$ ]; Rc, biomass density of the layer of crowns [ $\text{t ha}^{-1} \text{m}^{-1}$ ].

measured at the height of  $H_3$ . Furthermore, the measurements of the rainfall under the canopy as well as soil temperature (at 16 depths every 5 cm starting from the ground level) and soil humidity (4 levels at the depths from 5 cm to 90 cm, depending on a site) were also conducted. All data were logged simultaneously at all levels every 6 min (averaging time) for up to 8 days, but separately for each site. The measuring equipment was mounted directly to a stem with no any damage to the canopy structure. The scheme of the gauging section inside mature seed forest is shown in Fig. 2 (left). Three-cup anemometers, with the cup diameter of 60 mm, were used to gauge wind speed. The sampling instruments were calibrated in an open circuit aerodynamic tunnel at 8 points within the speed range of 0.1–20 m/s. The initial velocity was 0.35 m/s and the end speed was 0.28 m/s. The calibration procedure showed the linear characteristic of the anemometer with the determination coefficient of  $100 \cdot R^2 = 99.986\%$ , standard deviation of  $\sigma = 0.08$  and an average error of estimation equal to  $\mu = 1.06\%$ . Measurements were automatically taken every 6 min with a resolution of 0.1 m/s. Example data of the wind speed, obtained at site S4 (mature stand) at different heights, are shown in Fig. 2 (right). The average values of measured wind velocity are presented in Table 3. Due to the very small tallness of the tree stand at the site U (0.8 m, natural seeding) there were no measurements at the heights of  $H_2$  (just under the tree canopy) and  $H_3$  (about 2.2 m above the ground). Inside the thicket (site S1) it was impossible to distinguish a stem layer, hence wind speed data  $U_3$  and  $U_4$  were *de facto* obtained within the crown layer.

A characteristic variation is well noticeable on presented waveforms of wind velocity – when the wind speed over treetops ( $U_1$ ) is sufficiently high ( $U_1 > 1.5 \text{ m/s}$ ) then the wind velocity plots in the stem layer become disjointed (Fig. 2, see plots on the 2nd of August 2004). For light wind above the crown layer wind velocity plots in the stem layer are very similar (Fig. 2, see plots on the 31st of July 2004). In addition, it is possible to distinguish an increase of wind speed during a day, which may be caused by thermal movement of air on valley slopes (high temperature differences with the reference to the valley floor,

see plots on the 2nd of August 2004). Under the assumption that the roughness length  $h_{z0} = 0$  in Eq. (1), it is possible to plot characteristic S-shaped distributions of relative wind speed within tree stands (Fig. 3). One may suppose that observed changeability of wind speeds at different levels is the result of the uneven layered-oriented vertical distribution of the biomass inside the tree stands as well as determined by the position and the orientation of the analyzed surfaces located on valley slopes (i.e. tilt and azimuth angles, altitude, etc.). The wind velocity is strongly attenuated within the crown layer by the huge amount of biomass collected in the crown layer. At the sites U (natural seeding) and S1 (thicket) the wind speed was completely suppressed inside the crown layer. Inside maturing stands the values of the wind speed within stem layer were equal to about 30% of the wind speeds over the stands, but inside mature forests it grew to about 55%. ‘Roughness’ at the edges of the stem layer – the canopy bottom surface from the top and the forest litter from the bottom – also diminished the wind velocity. That is why the secondary maximum can be expected at the height of up to several metres. The number of trees per hectare can be an additional factor, which attenuates wind speed inside a forest community – at the height of 2.4 m the wind velocity within maturing stands (sites M and S2) is smaller than within mature forests (sites L, F and S4), 40–45% and 55% of a wind speed over the stands respectively. At the site O (mature forest), the observed waveform of the vertical wind velocity distribution did not unambiguously reveal the existence of the secondary maximum. This situation could have resulted from the lack of the dry state under the canopy as a consequence of the already finished dead branch self-pruning process, or on the other hand, of the location of this research site just near border of the catchment area (Fig. 1), which followed the Ridge of Bukowiec Mountain (750 m AMSL). In such a case this site could have been over-exposed to a wind force considerably stronger than to other sites (not only from the ‘heart’ of the valley). At site H (the oldest maturing stand) the wind velocity attenuation under canopy was considerably bigger than at other maturing stands (sites M and S2) and was very similar to the attenuation observed in seed stands

**Table 3**  
Wind speed gauged at the investigated sites.

Site	$\bar{U}_1$	Range	$\bar{U}_2$	Range	$\bar{U}_3$	Range	$\bar{U}_4$	Range
U	0.52	0.04–1.10	–	–	–	–	0.00	0.00–0.00
S1	0.58	0.00–0.95	–	–	0.00	0.00–0.04	0.00	0.00–0.00
M	0.97	0.44–1.39	0.27	0.00–0.56	0.37	0.09–0.64	0.18	0.00–0.48
S2	0.63	0.20–1.21	0.08	0.00–0.51	0.28	0.04–0.58	0.11	0.00–0.61
H	0.76	0.34–1.31	0.30	0.00–0.52	0.47	0.18–0.55	0.49	0.13–0.61
O	0.88	0.22–1.90	0.48	0.00–0.74	0.45	0.04–0.82	0.35	0.00–0.71
L	1.02	0.18–1.54	0.44	0.00–0.60	0.56	0.09–0.82	0.39	0.04–0.57
F	0.93	0.32–1.88	0.34	0.00–0.59	0.50	0.05–1.04	0.28	0.00–0.67
S4	1.29	0.47–2.63	0.58	0.00–0.95	0.72	0.17–1.50	0.55	0.04–1.14

$\bar{U}_i$  is an average wind speed at the height  $H_i$  (Table 1) [m/s].

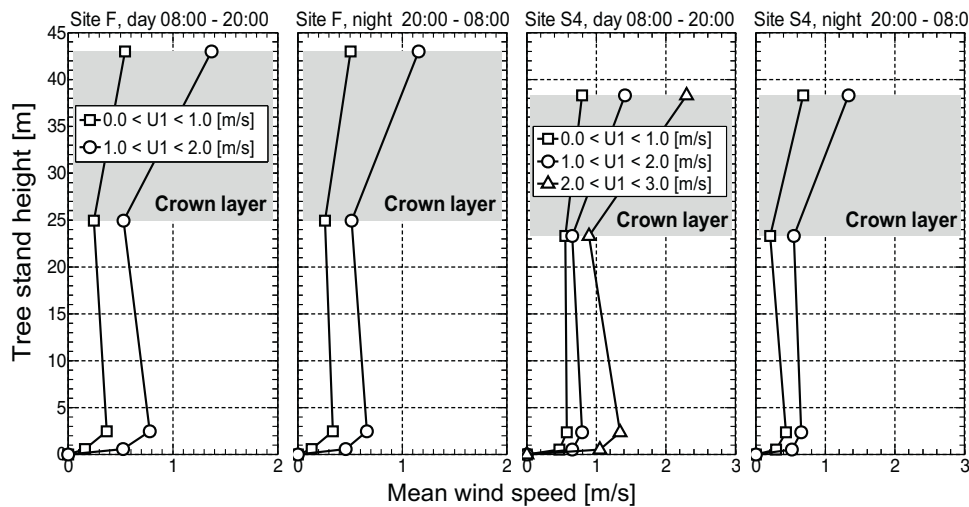


**Fig. 4.** Vertical wind speed profiles for conditionally sampled data at sites F and S4 (mature stands). The S-shaped wind speed profile may be observed in all considered cases: different ranges of the average wind speed above the tree tops ( $U_1$ ) as well as during day (08:00–20:00) and at night (20:00–08:00).

(sites L, F and S4). Inside mature forests all S-shaped wind speed profiles were very similar to each other, except for the site O. At all research site gauged wind velocity distributions significantly differed from the classical logarithmic shape, defined by Eq. (1).

### 3. Wind profile model

The standard mixing length theory, which assumes downward momentum transfer and negative wind gradient  $\partial \bar{u} / \partial h$ , works only in young stands (sites U and S1). There was no stem layer thus the mean wind speed was totally suppressed inside the canopy. In older stands when the stem layer was distinguishable it has been observed that all gradient-diffusion schemes fail completely (Denmead and Bradley, 1985; Yi, 2008). The formation of a stem layer within spruce stands is a very complicated process (Czarnowski, 1978). Simplifying, a stem layer is formed in a dense coniferous forest complex by withering and self-falling of the lowest branches. Next, as the result of this multiannual dead branch self-pruning process, a 'clear' trunk space appears between the ground and 'green' branches in the crown layer. Nevertheless, dry branches are present inside the stem layer of maturing stand for long time (sites M, S2 and H). The amount and spatial density of this dry state depends mainly on the age of tree stand and also on the site index. Such dry branches are often cut off by foresters to improve the stem quality. In mature stands (sites L, F and S4) the dry state can be practically omitted. The secondary maximum may be observed regardless of conditionally data sampling: different ranges of the average wind speed above the tree tops as well as for day and night (Fig. 4). Analogous patterns are detected in the one-dimensional laminar steady flow inside a homogeneous environment between parallel surfaces whose size is assumed to be very large compared with their separation distance. The shape of the mean speed is parabolic and the maximum velocity occurs at the centreline between two plates (Currie, 2003). The recorded S-shaped profile in real forests is asymmetric (Queck and Bernhofer, 2010; Yi, 2008) because of the dry state in the upper part of the trunk space (there were neither shrub layer nor forest vegetal cover at the investigated stands). The existence of the secondary maximum leads to a conclusion that, except for downward momentum transfer, there might be an additional air flow within the stem layer just over the soil surface. This flux might be driven by an input flow across a forest edge. It is known that the wind speed in the stem layer is expressed by an exponential decay function with distance from the forest edge and a rapid adjustment,

which is essentially complete by about  $x = 10H$  from the forest edge (Lee, 2000 after Shinn, 1971 and McNaughton, 1989). Although the basin was densely afforested, there were some forest clearings and felling sites (about of 5% of the catchment area) and forest roads (width: from 2 m to 4.5 m). The total length of roads was 7 km and the total road surface in the drainage area was 22,548 m<sup>2</sup> (road density index 41.7 m ha<sup>-1</sup>). It is necessary to notice that an even-aged homogenous tree stands were only within the particular precincts of site locality class, which area varied between several and 20 ha.

#### 3.1. Vertical wind profile under canopy

By analogy of data analyses in meteorology, average values of wind velocity within the period of 1 h were calculated based on gauged data. In this way, the number of cases essential to identify empirical models was increased. A wind speed has a random character and it is independent of the time of the day, like for instance the intensity of solar radiation or air temperature. Nevertheless, one ought to keep in mind that air mass movement over valley slopes may be driven by high temperature differences between the valley top and the valley bottom. It can be expected that the model equation should be based on the solution function of a differential equation of at least the second order. The differential equations describing the momentum transfer can be solved only under various simplifications, e.g. steady state, one dimensional flow or uniform vertical distribution of leaf area (biomass) and drag coefficient (Inoue, 1963; Zeng and Takahashi, 2000; Yi, 2008). Furthermore, such models would be defined, in general case by 4 or even more parameters and could not be verified based on limited measurements, such as in this research. The observed wind speed pattern is asymmetrical and the secondary maximum is located in the lower part of the stem layer (Queck and Bernhofer, 2010, their Fig. 3 (left), Yi, 2008, his Fig. 1 (left)) and it can be defined by the following empirical formula, which is often used in technical modelling:

$$U(h) = \alpha \cdot h^\beta \cdot e^{-\gamma \cdot h}, \quad (4)$$

where  $U(h)$  is the wind velocity [m/s] at the height of  $h$  [m],  $\alpha$ ,  $\beta$  and  $\gamma$  are the coefficients to be calculated during the identification of the model equation (4). The  $\alpha$  parameter is the gain coefficient, parameters  $\beta$  and  $\gamma$  are responsible for the increase of the wind speed near the ground and for the decline of the wind velocity in the trunk space. The function Eq. (4) can be used in forest practice only

**Table 4**  
Average regression statistics for Eq. (4) with calculated values of Eqs. (5) and (6).

Site	$\alpha$	$\beta$	$\gamma$	$U_m$	$H_m$	$H_m/H_s$	$R$	100· $R^2$	$\sigma$	$\mu$	$Q_1$	$Q_3$
M	0.321	0.708	0.203	0.38	3.48	0.41	1.000	100.00	0.004	1.63	0.58	−2.38
S2	0.336	1.233	0.521	0.28	2.37	0.31	1.000	100.00	0.002	1.52	−0.14	−3.37
H	0.576	0.146	0.133	0.50	1.10	0.15	1.000	99.98	0.002	0.50	0.55	−0.29
O	0.421	0.158	0.020	0.50	7.86	0.56	0.999	99.90	0.004	0.83	0.94	−0.45
L	0.480	0.316	0.044	0.65	7.14	0.28	1.000	100.00	0.004	0.94	0.87	−0.46
F	0.386	0.485	0.068	0.62	7.12	0.28	1.000	99.99	0.002	0.52	0.66	−0.20
S4	0.651	0.219	0.035	0.78	6.32	0.27	1.000	100.00	0.001	0.16	0.15	−0.09

$R$ , correlation coefficient;  $\sigma$ , standard deviation of estimation;  $\mu$ , average error of estimation;  $Q_3$ , upper quartile;  $Q_1$ , lower quartile.

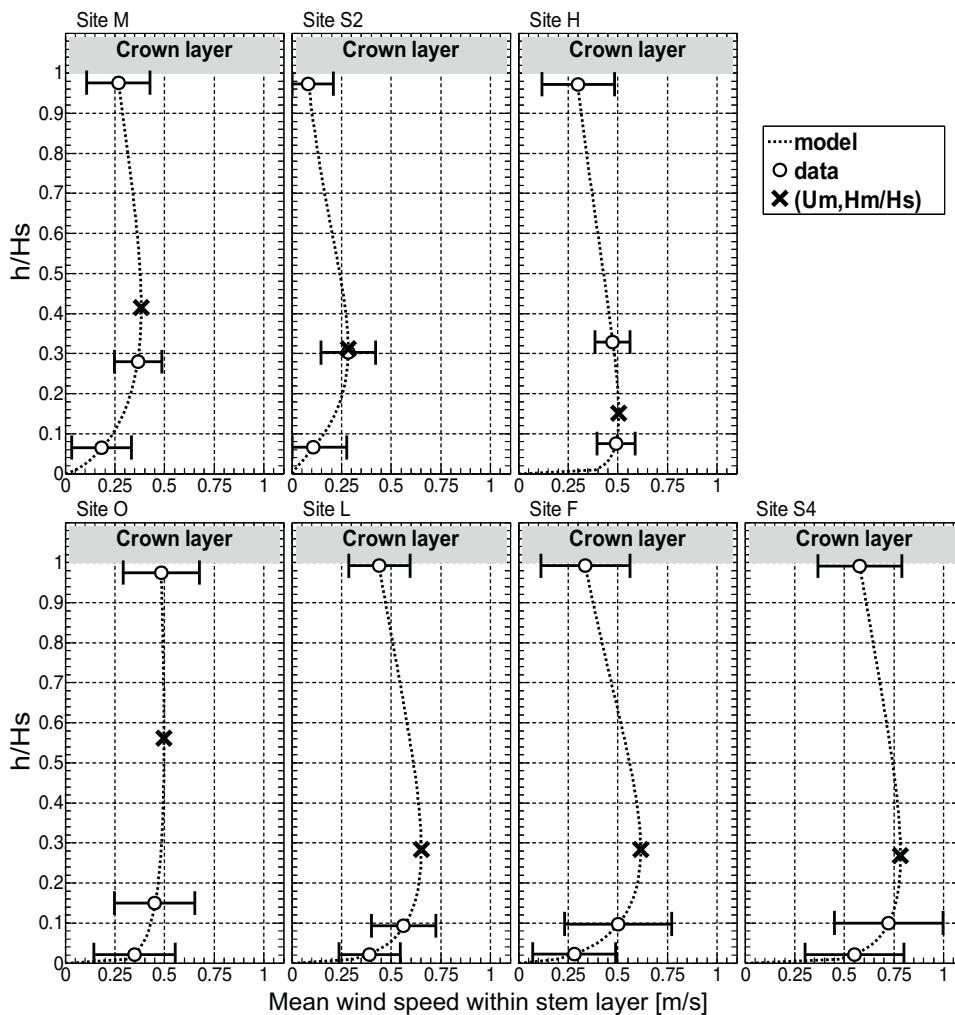


**Fig. 5.** Vertical wind speed profiles within stem layer obtained by presented model in investigated stands. The vertical axis is normalized height with reference the height of the stem layer ( $H_s$ ). Cross markers indicate calculated values of the maximal wind speed within the stem layer ( $U_m$  at the height  $H_m$ , see Table 4). For mature forests (sites L, F and S4) and for one maturing stand (site S2) the maximal wind velocity under the canopy occurred at the height of about 28% of the height of the stem layer. It is possible to formulate a hypothesis that the value of  $H_m$  is constant and it is characteristic to the particular species (there was no distinguishable relation to neither measured or calculated biometric features of tree stands nor their combinations).

**Table 5**  
Regression statistics for  $p = U_m/U_1$ .

Site	$K$	$p$	95% CI	$R$	100· $R^2$	$\sigma$	$\mu$	$Q_3$	$Q_1$
M	36	0.396	0.361–0.431	0.64	40.85	0.11	26.58	16.52	−11.61
S2	54	0.447	0.412–0.482	0.47	22.55	0.13	43.62	31.41	−40.24
H	20	0.668	0.609–0.727	0.72	51.67	0.13	25.33	23.98	−11.46
O	12	0.564	0.478–0.649	0.87	76.15	0.15	29.76	26.16	−22.38
L	41	0.640	0.593–0.688	0.63	39.93	0.15	23.40	21.94	−18.99
F	36	0.663	0.620–0.706	0.90	80.27	0.13	20.80	14.23	−11.88
S4	87	0.606	0.577–0.634	0.87	76.43	0.14	17.28	10.13	−9.54

$K$ , number of cases;  $p = U_m/U_1$ , regression coefficient; CI, confidence intervals;  $R$ , correlation coefficient;  $\sigma$ , standard deviation of estimation;  $\mu$ , average error of estimation;  $Q_3$ , upper quartile;  $Q_1$ , lower quartile.

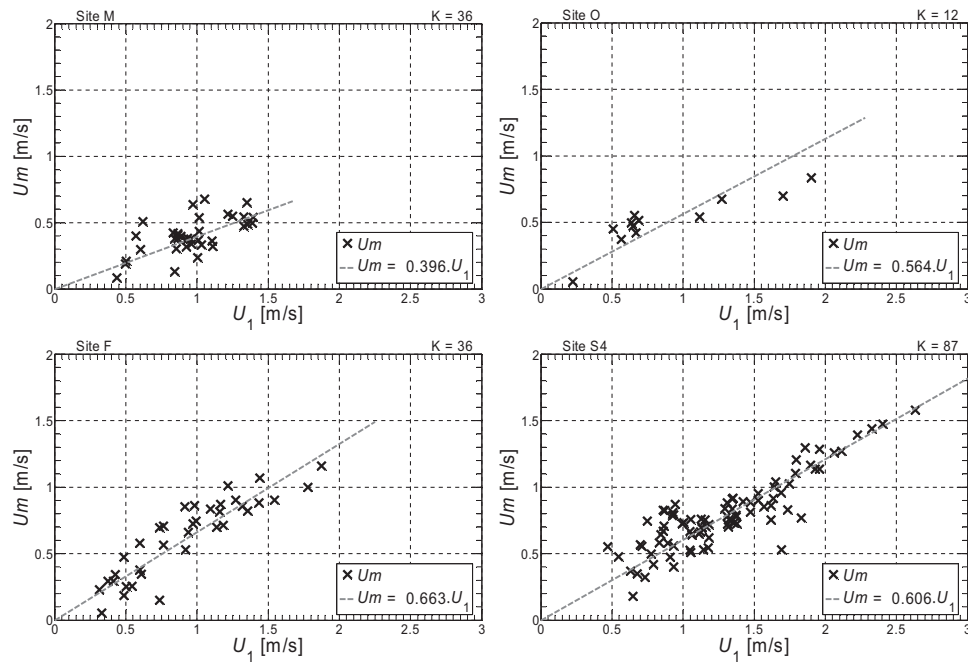


**Fig. 6.** Relationships between wind speed over tree tops ( $U_1$ ) and calculated values of the maximal wind speed within the stem layer ( $U_m$ ).  $K$  indicates the number of cases. The different values of the linear regression coefficient  $p = U_m/U_1$  denote different attenuation of wind speed within the crown layer at different investigated sites. The highest suppression is observed in the young maturing stand (site M), the lowest reduction of the wind speed is in mature stands (sites L, F and S4). It may be explained, in comparison to mature stands, by a considerably higher number of trees per hectare and biomass density in the crown layer (see Table 2).

when all parameters  $\alpha$ ,  $\beta$  and  $\gamma$  will be expressed by the biometric features of tree stands. The results of identification of the formula Eq. (4) are presented in Table 4. However, the results of the test of goodness of fit are very high, one should take into consideration that the coefficients  $\alpha$ ,  $\beta$  and  $\gamma$  were estimated using only three values of the wind velocity. The regression statistics confirm that the form of Eq. (4) was correctly matched and, according to values of the correlation coefficient  $R$  or  $100 \cdot R^2$ , the variability of  $U(h)$  may be explained with high accuracy. Only in these cases, where the correlation coefficients higher than 99% (Table 4) and the calculated values of  $H_m$  (defined in Section 3.2, Eq. (5)) inside the stem layer, were taken into future consideration. The vertical distribution of the wind velocity inside the stem layer with the normalized height to the elevation of the crown layer, according to the Eq. (4), is shown in Fig. 5. In all estimated curves, the secondary maximum of wind speed is well noticeable and is denoted by a cross marker.

### 3.2. Secondary wind speed maximum within stem layer

The model function Eq. (4) at the height of:

$$H_m = \frac{\beta}{\gamma}, \tag{5}$$

reaches its maximal value:

$$U_m = \alpha \cdot \left(\frac{\beta}{\gamma}\right)^\beta \cdot e^{-\beta}, \tag{6}$$

**Table 6**  
Regression statistics for Eq. (7).

$\delta$	95% CI	$R$	$100 \cdot R^2$	$\sigma$	$\mu$	$Q_3$	$Q_1$
0.0754	0.0742–0.0766	0.999	99.73	0.008	1.417	0.61	-0.27

CI, confidence intervals;  $R$ , correlation coefficient;  $\sigma$ , standard deviation of estimation;  $\mu$ , average error of estimation;  $Q_3$ , upper quartile;  $Q_1$ , lower quartile.

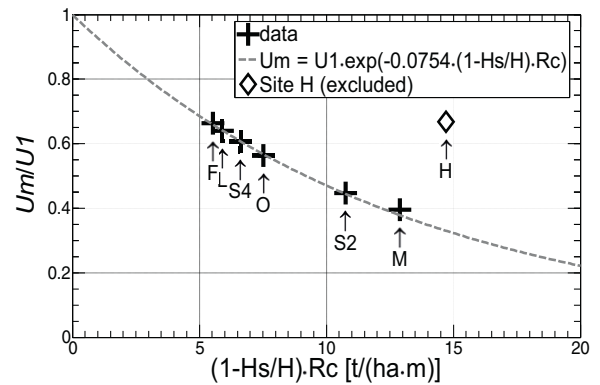


**Fig. 7.** Relationships between maximal wind speed within stem layer ( $U_m$ ) and wind speed over tree tops ( $U_1$ ) as a function of biometric features of tree stand: biomass density in the crown layer ( $R_c$ , fresh mass only, see Table 2), an elevation of the crown layer (the height of the trunk space,  $H_s$ ) and the height of the tree stand ( $H$ ).

where  $\alpha$ ,  $\beta$ ,  $\gamma$  are defined like in Eq. (4). According to the hypothesis that the vertical wind profile is mainly shaped by the tree stands forested in the research sites, the calculated parameters  $H_m$  and  $U_m$  (Table 4; Fig. 5) by using Eqs. (5) and (6), should depend on their biometric features. Fig. 6 presents the relationship between the maximal wind velocity within stem layer  $U_m$  and the wind speed above the crown layer  $U_1$ . The changeability of computed data may suggest that there is the linear dependence between these wind velocities  $U_m = p \cdot U_1$ . The results of such identification are presented in Table 5. It can be noticed that different values of the linear regression coefficient  $p = U_m/U_1$  denote different attenuation of wind speed within the crown layer at different investigated sites. The highest suppression can be observed in the young maturing stand (site M), the lowest reduction of the wind speed is in mature stands (sites L, F and S4). It may be explained, in comparison to mature stands, by a considerably higher number of trees per hectare and biomass density in the crown layer (Table 2). It



**Table 7**  
Regression statistics for identification of linear relationship between gain coefficient ( $\alpha$ ) and total basal area (see Fig. 8).

$\lambda$	$\xi$	Root	$R$	100· $R^2$	$\sigma$	$\mu$	$Q_3$	$Q_1$	
0.0176	-0.3029	17.2	0.980	96.04	0.029	5.75	4.19	-4.41	Sites S2, H, O, S4
0.0238	-0.7770	32.6	0.910	82.85	0.033	8.36	5.06	-6.45	Sites M, F, L

$R$ , correlation coefficient;  $\sigma$ , standard deviation of estimation;  $\mu$ , average error of estimation;  $Q_3$ , upper quartile;  $Q_1$ , lower quartile.

should be noticed that all measurements were running for only a few days at each site (see Table 1, column DY), therefore the diversity of the wind speed over treetops  $U_1$  was rather small. In this case, the relationships presented in Fig. 6 may be only approximated by a linear function in a limited domain. Inside the mature forest, in the presence of higher changeability of wind velocities  $U_1$  and  $U_m$ , the interpolation errors are considerably lower.

The wind speed within the canopy is usually modelled as an exponential function of cumulative leaf drag area per unit planform area (Massman, 1997) or LAI (Inoue, 1963; Yi, 2008). Due to the observation that the value of the coefficient  $p$  (Table 5) is inversely proportional to the biomass density in the crown layer (Table 2,  $R_c$ ), it could be expected that the biomass density may be equivalent to the leaf area density. Furthermore, it can be supposed that an elevation of the crown layer (the height of the trunk space) may have an influence on the wind speed attenuation (Fig. 3). Based on such hypotheses and assuming that  $U_m = U_1$  for  $R_c = 0$  (no tree stand) the following formula was empirically derived:

$$U_m = U_1 \cdot \exp \left\{ -\delta \cdot R_c \cdot \left( 1 - \frac{H_s}{H} \right) \right\}, \quad (7)$$

where  $U_1$  is the wind speed over treetops [m/s];  $U_m$  is the maximal wind speed within the stem layer [m/s];  $U_s$  is the height of the stem layer [m];  $H$  is the height of the tree stand [m];  $R_c$  is the biomass density within the crown layer [ $\text{t ha}^{-1} \text{m}^{-1}$ ] (Table 2);  $\delta$  is the coefficient to be estimated during the identification of Eq. (7). The form of the above formula is very similar to Eq. (2), proposed by Yi (2008). The regression statistics of identification of Eq. (7) are presented in Table 6 and in Fig. 7. The site H differed from the others thus was excluded from the calculations. This exception of the rule may have been caused by wrongly estimating biomass density in the canopy. It also should be taken into consideration that due to the age of the tree stand (41 years old) at this site, the dead branch self-pruning process may have been nearly finished inside the trunk space. That is why  $U_m$  at this site is similar to the values calculated in mature forests than in other maturing stands.

The analysis of the changeability of the height of the occurrence of the maximum wind speed within the stem layer ( $H_m$  in Table 4) did not reveal any relation to neither measured or calculated biometric features of tree stands nor their combinations. According to the results presented in Fig. 5 and in Table 4 it is possible to formulate a hypothesis that the value of  $H_m$  is constant and it is characteristic to the particular species. For mature forests (sites L, F and S4) and for one maturing stand (site S2) the maximal wind velocity under the canopy occurred at the height of about 28% of the height of the stem layer. The differences for the sites M and H may be explained by the incorrect (overstated) measurements of  $U_2$  or  $U_4$  respectively. Yet the mean value for these two sites is still equal to 28%. The divergence for the site O can be clarified by the localization of this site (just under the Ridge of Bukowiec Mountain, Fig. 1) and its exposure to possibly stronger winds compared to other experimental sites.

### 3.3. Gain coefficient (parameter $\alpha$ )

The gain coefficient  $\alpha$  in Eq. (4) demonstrates a linear relationship to the total basal area ( $\alpha = \lambda \cdot TBA + \xi$ ), presented in Fig. 8. The sites located just over the valley floor (sites M, L and F) have a

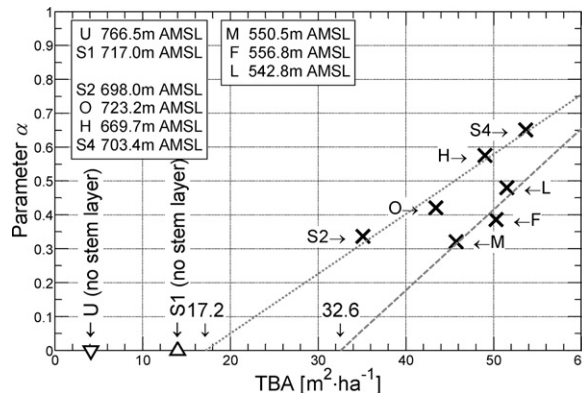


**Fig. 8.** Relationship between gain coefficient  $\alpha$  of the presented model and total basal area ( $TBA$ ) of the investigated tree stands. The sites located just over the valley floor (dashed line, sites M, L and F, see Table 1) have a different (higher) value of the slope coefficient (see Table 7) than sites with high relative elevations (dotted line, sites S2, H, O and S4, see Table 1). The ratio of the empirically estimated roots of these linear regressions ( $32.6/1.72 \cong 1.89$ ), is approximately the same as the ratio of the altitudes of the highest and the lowest points in the valley, where the catchment was located ( $Zvt/Zvf = 881.9/477.5 \cong 1.85$ ). The wind speed was totally attenuated in the natural seeding (site U) and the thicket (site S1), thus it was assumed that  $\alpha = 0$  (see Table 3 and Fig. 3).

different (higher) value of the slope coefficient  $\lambda$  (Table 7) than sites with high relative elevations (sites S2, H, O and S4). There was no stem layer at the research site U and S1; therefore it is impossible to define the value of the parameter  $\alpha$  correctly. It may be postulated that the parameter  $\alpha$  ought to be equal to zero for these two sites, because the wind speed was completely attenuated within the canopy (Table 3; Fig. 3).

The relationships presented in Fig. 8 and Table 7 suggest that the gain coefficient also depends on the elevation to the valley floor. Furthermore, it may be noticed that the ratio of the empirically estimated roots of this linear regression (Fig. 8),  $32.6/1.72 \cong 1.89$ , is approximately the same as the ratio of the altitudes of the highest and the lowest points in the catchment area (valley)  $Zvt/Zvf = 881.9/477.5 \cong 1.85$ . The collision point of these two straight lines is for the  $TBA = 76.22$  and the parameter  $\alpha$  is equal to  $1.04 \approx 1$ . Hence, the parameter  $\alpha$  in Eq. (4) can be calculated taking into consideration the total basal area with the adjustment to the relative elevation of the sites above the local valley bottom with the reference to the valley prominence (Tables 1 and 2):

$$\alpha = \lambda \cdot \frac{TBA}{(Zvt/Zvf) - (Zrl/dZv)} + \xi \quad (8)$$

where  $TBA$  is the total basal area [ $\text{m}^2 \text{ha}^{-1}$ ];  $Zvt$  is the altitude of the highest point inside the catchment area (valley) [m];  $Zvf$  is the altitude of the lowest point inside the catchment area (valley) [m];  $dZv$  is the valley prominence [m];  $Zrl$  is the relative elevation to the local valley floor or to the altitude of the recession point of the

**Table 8**  
Regression statistics for Eq. (8).

$\lambda$	$\xi$	Root	$R$	100· $R^2$	$\sigma$	$\mu$	$Q_3$	$Q_1$
0.0287	-0.3670	12.8	0.955	91.10	0.037	8.14	8.14	-8.44

$R$ , correlation coefficient;  $\sigma$ , standard deviation of estimation;  $\mu$ , average error of estimation;  $Q_3$ , upper quartile;  $Q_1$ , lower quartile.

**Table 9**  
Regression statistics for Eq. (9).

$\lambda$	$\xi$	Root	R	100·R <sup>2</sup>	$\sigma$	$\mu$	Q <sub>3</sub>	Q <sub>1</sub>	
-0.0544	3.1629	58.1	0.994	98.89	0.043	7.17	6.29	-12.10	Slope coeff. ( $\beta$ )
-0.0276	1.4792	53.6	0.993	98.57	0.022	13.16	4.38	-31.33	Attenuation coeff. ( $\gamma$ )

R, correlation coefficient;  $\sigma$ , standard deviation of estimation;  $\mu$ , average error of estimation; Q<sub>3</sub>, upper quartile; and Q<sub>1</sub>, lower quartile.

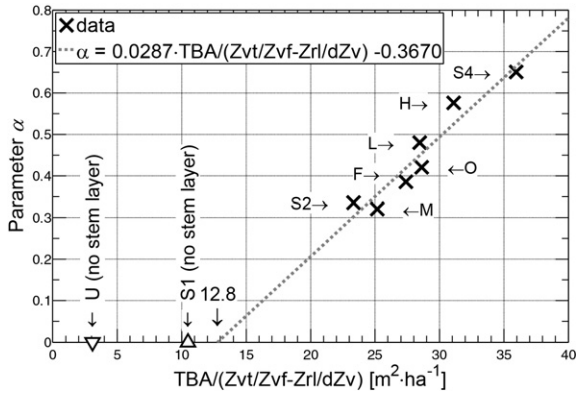


**Fig. 9.** Relationship between gain coefficient  $\alpha$  of the presented model and total basal area ( $TBA$ ) with the empirical correction for the relative elevation of the sites above the local valley bottom with respect to the valley prominence (see Table 1):  $Zvt$  is the altitude of the valley top,  $Zvf$  is the altitude of the valley floor,  $Zrl$  is the relative elevation of the investigated site with the reference to the local valley floor or to the altitude of the recession point of the valley bottom gradient, and  $dZv$  is the valley prominence. The wind speed was totally attenuated in the natural seeding (site U) and the thicket (site S1), thus it was assumed that  $\alpha=0$  (see Table 3 and Fig. 3). The estimated root may suggest that the trunk space can be distinguished within a spruce tree stand when  $TBA$  is greater than  $\sim 12.8$ .

valley bottom gradient [m] (Table 1);  $\lambda, \xi$  are the coefficients to be estimated during identification of Eq. (8). The empirical correction coefficient, the denominator in Eq. (8), makes the allowance for the real elevation of the research sites over the local valley bottom relatively to the valley height. The regression statistics for identification of Eq. (8) are presented in Table 8 and in Fig. 9.

**3.4. Slope and attenuation coefficients (parameters  $\beta$  and  $\gamma$ )**

The parameters  $\beta$  and  $\gamma$  occurring in the model Eq. (4) are responsible for the wind speed increase just over the ground and the wind speed attenuation under the crown layer. According to conditions occurring in the research sites the wind speed pattern should depend on biometric characteristics of stems only. These both parameters, similarly to the parameter  $\alpha$ , also reveal a linear relation to the total basal area ( $TBA$ ), presented in Fig. 10:

$$\{\beta, \gamma\} = \lambda \cdot TBA + \xi \tag{9}$$

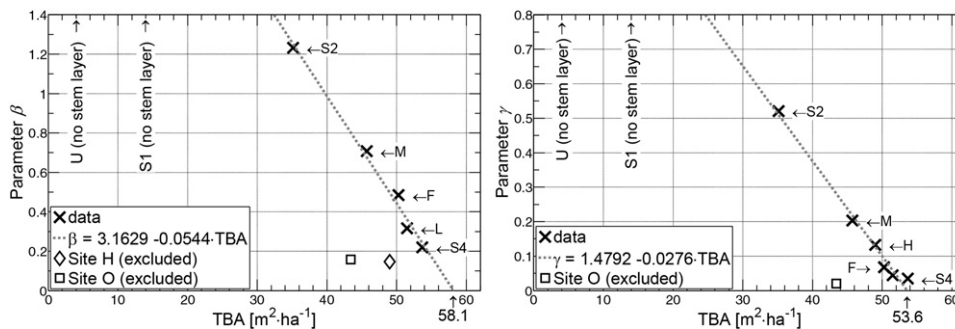


**Fig. 10.** Relationship between total basal area ( $TBA$ ) and slope coefficient  $\beta$  (left) and attenuation coefficient  $\gamma$  (right) of the model equation. The high values of the parameters at the site S2 may be explained by a great amount of withered branches within the trunk space. Such dry state is characteristic of the dead branch self-pruning process which forms the stem layer inside coniferous stands. In contrast, at the sites located in mature stands the low values of parameter  $\gamma$  describe slight wind speed attenuation under the crown layer (see Fig. 5). The wind speed was totally attenuated in the natural seeding (site U) and the thicket (site S1), thus under the assumption  $\alpha=0$  (see Eq. (4) and Fig. 9) the values of parameters  $\beta$  and  $\gamma$  are undetermined for these sites.

**Table 10**  
Regression statistics for Eq. (11).

$\varepsilon$	95% CI	R	100·R <sup>2</sup>	$\sigma$	$\mu$	Q <sub>3</sub>	Q <sub>1</sub>
0.0972	0.0648–0.1294	0.978	95.56	0.044	10.93	8.59	-16.97

CI, confidence intervals; R, correlation coefficient;  $\sigma$ , standard deviation of estimation;  $\mu$ , average error of estimation; Q<sub>3</sub>, upper quartile; Q<sub>1</sub>, lower quartile.

where  $TBA$  is the total basal area [ $m^2 ha^{-1}$ ];  $\lambda, \xi$  are the coefficients to be estimated during identification of Eq. (9). The high values of the parameters  $\beta$  and  $\gamma$  at the site S2 may be explained by a great amount of withered branches in the trunk space, which hampers the air flow in this layer (Fig. 5). In contrast, at the sites located in mature stands the low values of the parameter  $\gamma$  describe slight wind speed attenuation under the crown layer. It can be also observed that the wind speed increase near the ground at the sites H and O is violent (Fig. 5), thus the values of the parameter  $\beta$  are very small. Furthermore, at the site O there was practically no wind velocity attenuation connected with the change of the height. That is why these two sites were excluded from the analysis. The regression statistics for identification of Eq. (9) are presented in Table 9 as well as in Fig. 10.

**3.5. Average wind speed within stem layer**

Empirical equations describing the water budget in the atmosphere – tree stand – soil system usually consider the wind velocity above and within tree stand (Suliński and Starzak, 2009). The mean wind speed within the stem layer, formally based on the integrating of Eq. (4), can be calculated by the following formula:

$$\begin{aligned} \bar{U} &= \frac{1}{H_s} \int_0^{H_s} \alpha \cdot h^\beta \cdot e^{-\gamma \cdot h} dh \\ &= \frac{\alpha}{(\beta + 1) \cdot \gamma} \cdot (H_s)^{\beta-1} \cdot (\gamma \cdot H_s)^{\beta/2} \cdot e^{1/2 \cdot \gamma \cdot H_s} \cdot \text{WhittakerM} \left\{ \frac{\beta}{2}, \frac{\beta + 1}{2}, \gamma \cdot H_s \right\} \end{aligned} \tag{10}$$

where:  $H_s$  is the height of the stem layer [m];  $\alpha, \beta, \gamma$  are the coefficients defined like in Eq. (4); WhittakerM is the function which satisfies Whittaker’s differential equation (Slater, 1972). By

**Table 11**  
Regression statistics for Eq. (12) – exponential model.

$\eta$	95% CI	R	100·R <sup>2</sup>	$\sigma$	$\mu$	Q <sub>3</sub>	Q <sub>1</sub>	
0.1099	0.0831–0.1367	0.814	66.22	0.059	39.57	21.11	–57.54	Sites H, S1 excluded

CI, confidence intervals; R, correlation coefficient;  $\sigma$ , standard deviation of estimation;  $\mu$ , average error of estimation; Q<sub>3</sub>, upper quartile; Q<sub>1</sub>, lower quartile.

**Table 12**  
Regression statistics for Eq. (13) – linear model.

$\lambda$	$\xi$	Root	R	100·R <sup>2</sup>	$\sigma$	$\mu$	Q <sub>3</sub>	Q <sub>1</sub>	
0.0178	–0.5066	28.4	0.978	95.58	0.025	7.45	6.27	–7.53	Site O excluded

CI, confidence intervals; R, correlation coefficient;  $\sigma$ , standard deviation of estimation;  $\mu$ , average error of estimation; Q<sub>3</sub>, upper quartile; Q<sub>1</sub>, lower quartile.

the analogy to the calculation of the maximum wind speed under the canopy ( $U_m$ , Eq. (7)), the mean wind velocity ( $\bar{U}$ , Eq. (10)) can be computed by applying an exponential function with the allowance for the biomass density within the canopy and the elevation of the crown layer:

$$\bar{U} = U_1 \cdot \exp \left\{ -\varepsilon \cdot R_c \cdot \left( 1 - \frac{H_s}{H} \right) \right\}, \quad (11)$$

where  $U_1$  is the wind speed over the treetops [m/s],  $H_s$  is the height of the stem layer [m];  $R_c$  is the biomass density of the crown layer [t (ha m<sup>-1</sup>)];  $\varepsilon$  is the coefficient to be estimated during the identification of Eq. (11). For the sites U and S1, where there were no stem layer, the momentum transfer was attenuated completely ( $U_4 = 0$ , Table 3), thus it may be assumed that the mean wind speed is equal to zero at these both sites. It also could be supposed that for the site S1 the biomass density was underestimated. Similarly to the previous analyses the site H differed from other maturing stands. Therefore these sites (S1 and H) were excluded from the analysis. The detailed results of the test of goodness of fit for Eq. (11) are presented in Table 10 and in Fig. 11

3.6. Wind attenuation within canopy

By the analogy to the maximal wind velocity within the trunk space (Eq. (7)) the wind speed just under the canopy can be estimated by an empirical, exponential function taking into consideration the biomass density within the canopy and the empirical correction coefficient of the crown layer thickness relative to the height of the tree stand:

$$U_2 = U_1 \cdot \frac{H}{H_c} \cdot e^{-\eta \cdot R_c}, \quad (12)$$

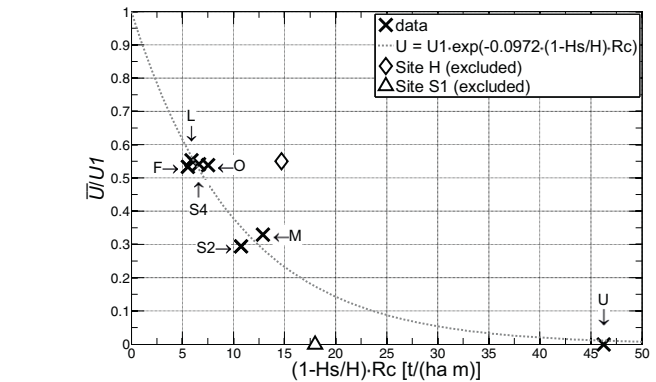
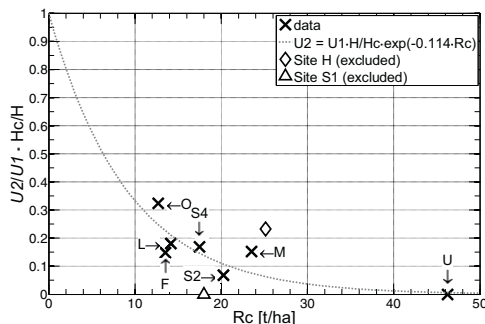


**Fig. 11.** Relationship between mean wind speed inside the trunk space ( $\bar{U}$ ) and wind speed over tree tops ( $U_1$ ) as a function of biometric features of tree stand: biomass density in the crown layer ( $R_c$ , fresh mass only, see Table 2), an elevation of the crown layer (the height of the trunk space,  $H_s$ ) and the height of the tree stand ( $H$ ). A high value of the mean wind velocity at the site H may be explained by already finished dead branch self-pruning process and the lack of the dry state under the canopy. There was no stem layer in the natural seeding (site U) and the thicket (site S1), thus  $\bar{U}$  was equal to zero (see Table 3 and Fig. 3).

where  $U_1$  is the wind speed over treetops [m/s];  $H$  is the height of the tree stand [m];  $H_c$  is the thickness (the height) of the crown layer [m];  $R_c$  is the biomass density inside the crown layer [t ha<sup>-1</sup> m<sup>-1</sup>];  $\eta$  is the coefficient to be estimated during identification of Eq. (12). Comparably to previously presented analysis the sites S1 and H are significantly different from the other sites and both were excluded again. Table 11 and Fig. 12 (left) show the regression statistics for Eq. (12). Besides of Eq. (12) the attenuation of momentum transfer within the canopy could be also expressed by the total basal area:

$$U_2 = U_1 \cdot (\lambda \cdot TBA + \xi), \quad (13)$$

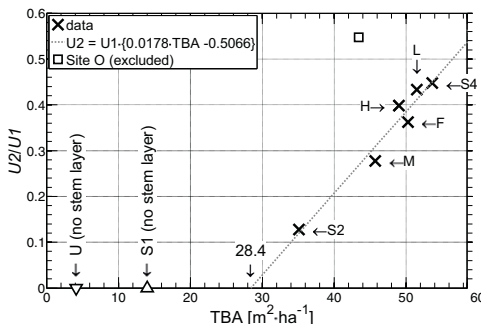


**Fig. 12.** Relationship between wind speed just under the canopy ( $U_2$ ) and wind speed over tree tops ( $U_1$ ) as a function of biometric features of tree stand. The left plot presents the dependence upon biomass density in the crown layer ( $R_c$ , fresh mass only, see Table 2), the thickness of the crown layer ( $H_c$ ) and the height of the tree stand ( $H$ ). The right graph depicts the relation to the total basal area ( $TBA$ ). There was no stem layer in the natural seeding (site U) and the thicket (site S1), thus  $U_2$  was equal to zero (see Table 3 and Fig. 3).

where  $U_1$  is the wind speed over treetops [m/s];  $TBA$  is the total basal area [ $\text{m}^2 \text{ha}^{-1}$ ];  $\lambda$ ,  $\xi$  are the coefficients to be estimated during the identification of Eq. (13). The regression statistics for the identification of Eq. (13) are presented in Table 12 and in Fig. 12 (right).

#### 4. Concluding comments

The presented empirical model provides an outline of the S-shaped vertical wind speed profile within the stem layer of Norway spruce stand (*Picea abies* (L) Karst., *ecotype – the Istebna spruce*). The main issue is a biological interpretation of the parameters  $\alpha$ ,  $\beta$  and  $\gamma$  in Eq. (4). A thorough understanding of all biological factors forming the observed S-shaped wind profile would considerably expand the knowledge of predicting the results of the silvicultural measures and a forest ‘ventilation’ process, which determines vaporization from the soil as well as the  $\text{CO}_2$  advection. It is possible to find in literature several models, which can generate the observed S-shaped distribution even with high precision, that are seldom based on the biometric features of tree stands (i.e. Lalic et al., 2003). A combination of two equations: Eq. (2) (Yi, 2008) inside the canopy and Eq. (4) within the stem layer enables to calculate the S-shaped wind speed profile in relation to the biometric features of a tree stand. The given, by Eq. (4), model describes the field-observed distribution with very high accuracy. However, it is essential to keep in mind that, due to technical conditions, wind speed data were obtained at just 3 levels within the stem layer. It means that a big part of this layer was not monitored, especially in mature forests. That is why the coordinates of the secondary wind velocity maximum ( $U_m, H_m$ ), calculated by Eqs. (4) and (5), can be underestimated (Table 4). Furthermore, although the whole experiment was running for 52 days, the measurements lasted a few days only (from 5 to 8 days) at each site (see Table 1, column DY); therefore the result may be inadequate to describe the situation for strong and extreme wind speeds. In this case, the presented relationships may be only approximated by a linear function in a limited domain. Nevertheless, it should be highlighted that all parameters used in Eq. (4) –  $\alpha$ ,  $\beta$  and  $\gamma$  – demonstrated a very high dependence on the biometric features of a given tree stand: the number of trees per hectare ( $N$ ), DBH and the altitudes of the research sites, which are effortlessly to be measured in the field (Table 8 and Table 9). Massman (1987), Massman and Weil (1999) and Yi (2008) found that wind speed attenuation within canopy is related to the LAI. At the research sites the LAI was equal to zero inside the stem layers. Thus, according to the presented analysis, the total basal area, based on only  $N$  and DBH, is the only factor determining how the wind speed increases over the ground (parameter  $\beta$ ) as well as the attenuation approaching the canopy (parameter  $\gamma$ ). The gain parameter  $\alpha$  in Eq. (4) additionally depends on the elevation above the local valley floor or above the recession point of the valley bottom gradient for the higher-elevated sites. The total basal area may be also used to evaluate the reduction of the wind velocity through the canopy Eq. (13).

It is necessary to underline that all biometric features of a tree stand ( $N, D, H, LAI$ ) as well as biomass ( $M_s, M_c$ ) or biomass density in a particular layer ( $R_s, R_c$ ) are dependent upon each other. Such relationships between these biometric features are the subject of interest in dendrometry (Fassnacht et al., 1994; Jonckheere et al., 2005; Turner et al., 2000). For instance, for the pine stands (*Pinus contorta* and *Pinus albicaulis*) there is a linear relationship between the LAI and sum of DBH (Suliński, 1993 based on data published by Karmanova et al., 1987; Peterson et al., 1989). In this case, the total basal area in a homogenous, even-age stand, automatically includes all information about the site quality, the biomass concentration within the different layers and the LAI. In addition, in contrast to

the  $TBA$ , the LAI is difficult to be measured precisely. There are two methods to determine the leaf area index: directly and indirectly based on photometrical measurements. The direct method requires stripping and measuring the foliage of the plant canopy samples. The disadvantage of the direct method is that it is destructive, time consuming and expensive, especially if the study area is very large. The disadvantage of the indirect method is that in some cases it can underestimate the value of LAI in very dense canopies, as it does not account for leaves that lie on each other, and essentially act as one leaf according to the theoretical LAI models (Wilhelm et al., 2000). The replacement of the LAI with the  $TBA$  would make the evaluation of the S-shaped wind speed profile easier.

In terms estimating the maximal and mean wind speed within the stem layer ( $U_m$  and  $\bar{U}$ , respectively), the biomass density inside the canopy and the elevation of the crown layer can be also used. The difference is only in the coefficient in the super-script in the exponential function. The exponential function directly refers to the analytical solutions of ordinary differential equations. In modelling, which takes ecological criteria into consideration, the exponential function works well to determine the momentum transfer within the canopy (Massman, 1987, 1997; Yi, 2008).

Another issue worth being investigated are the values of the total basal area for which Eqs. (8), (9) and (13) yield zero. It may be assumed, based on a comparison with the sites U and S1, that is a characteristic value, which determines the distinguishability of the stem layer. The estimated root (Eq. (8)) may suggest that the S-shaped wind pattern in the trunk space can be distinguished within a spruce tree stand when  $TBA$  is greater than  $\sim 12.8$ . A similar situation occurs to the parameters  $\beta$  and  $\gamma$  for the total basal area amount to 58.1 and 53.6, respectively, Eq. (9). In this case, when  $\beta = 0$  and  $\gamma = 0$ , according to Eq. (4), there is no the S-shaped wind speed profile within the stem layer, the values of  $U_m$  and  $H_m$  become undetermined. Corresponding to Eq. (13), the wind speed under the canopy  $U_2$  is greater than 0 for such tree stands, where  $TBA > 28.4$ . It should be remembered that all data were obtained in rather similar sites: 3 were located in maturing stands and 4 in mature forests; the choice of the research sites enabled to capture the differences resulting from the various locations on the valley slopes, but the diversity of the investigated tree stands was relatively small. Thus, the linear relationships – Eqs. (8), (9) and (13) – may only approximate more complex dependences, for example the sigmoid functions. Furthermore, the limited range of the explaining variable ( $TBA$ ) manifested in the large values of a standard deviation of the estimation ( $\mu$ ) and quartiles.

The characteristic S-shaped vertical wind speed profile was observed at all research sites, located inside homogenous, even-aged spruce stands. The oldest maturing stand at the site H (41 years old), nevertheless height-similar to other maturing stands M and S2 (Figs. 3 and 5), attenuated the wind velocity within the canopy (values of  $U_2$  and  $\bar{U}$ ) as in the mature seed forests (L, F and S4). This may have resulted from the already completed dead branch self-pruning process. The dry branches, located in the stem layer under the canopy, were not taken into consideration when estimating the biomass situated in the stem layer, yet had an influence on the acquired wind speed data. Such conditions were observed especially at the site S2 – the highest suppression ratio within the canopy 0.12. The tree stand at this research site demonstrated a very high attenuation of solar radiation (Suliński and Sypka, 2000), a lack of daily periodic temperature variation in the covering layer of soil (Sypka, 2003). The lowest suppression ratio within the canopy (0.55) was obtained at the site O, which was located near the border of the catchment, under the Ridge of Bukowiec Mountain. The direction of the wind was not monitored throughout this research, thus it was impossible to investigate the influence of the topographical aspects on the momentum transfer in the tree stands during the presented analysis.



The empirically calculated model, Eq. (4), suggests that the height of the occurrence of the secondary wind speed maximum ( $H_m$ ) can be constant and equal to about 28% of the height of the stem layer (Table 4). Some divergences may be notified for the sites M, H and O and be explained by either the incorrect (overstated) measurements of  $U_2$  or  $U_4$  respectively or by the localization of the site O. Based on the asymmetric S-shaped wind speed pattern within the trunk space, it is possible to formulate a hypothesis that the height of the secondary maximum depends on the different coarseness of the canopy bottom surface and the ground. According to complex canopy structure (branches, needles, dry state) the roughness grade of the crown bottom layer is higher than the roughness of the soil surface (there were neither shrub layer nor forest vegetative cover at the investigated stands). That is why the height of the secondary maximum is near the soil surface, not in the centreline between these two surfaces. On the other hand, it may be assumed that the value of  $H_m$  is a function of biomass density within the stem layer (Table 2); according to the chosen research sites such a postulate cannot be tested because the biomass density in the stem layer in the mature forests (O, L, F and S4) was practically the same and very similar to maturing stands (S2 and M).

Due to the type of investigated data, the postulated model may be applied to a homogenous, even-aged spruce tree stand. It is also essential to investigate whether the presented model may be used more generally and be applied to the uneven-aged or more complex tree stands. Such a parameterization scheme, taking into consideration the biometric features of a tree stand, which are uncomplicated to measure in the field (total basal area and tree stand height), should be easily transferable to stands composed of other tree species. The necessary improvements of the presented model may be possible after a series of measurements taken within various types of tree stands.

### Acknowledgements

We are grateful for the valuable comments and suggestions from Professor Józef Suliński from the Department of Forest Engineering, University of Agriculture in Krakow. We would like to also thank Dr. Jarosław Kucza from the Department of Forest Engineering for the excellent collaboration while completing this in-field research.

### Appendix. Calculations of biometric features of tree stand

The biometric features of a tree stand can be determined by field measurements of the number of trees per hectare ( $N$ ), DBH, the height of tree stand ( $H$ ) and the elevation of the canopy (the height of the lowest 'green' branches,  $H_s$ ). The necessary empirical equations were proposed by Suliński (1993, 2007). After calculating the mean DBH and the mean tree height of investigated stand by using Lorey's equation, the mean biomass of leaves of the mean tree ( $m_l$ ) may be calculated by the following empirical formula (Suliński, 2007):

$$m_l = 1.38 + 0.0766 \cdot \overline{DBH}^{1.71}, \quad (14)$$

where  $m_l$  is biomass of leaves of the mean model tree [kg],  $\overline{DBH}$  is the mean diameter at the breast height [cm]. The constant coefficients in Eq. (14) were identified based on data included in the yield tables (Schwappach, 1943). The volume of the trunk and branches of the mean model tree was estimated using the empirical equation:

$$v = 1.1 \cdot \overline{DBH}^{1.88} \cdot (H - 1.3)^{0.68}, \quad (15)$$

where  $v$  is the volume of the mean model tree (trunk and branches) [ $m^3$ ],  $\overline{DBH}$  is the mean diameter at the breast height [cm],  $H$  is the height of the mean model tree [m]. The constant coefficients in Eq. (15) were evaluated based on data published in the volumetric

tables (Czuraj et al., 1966). The total biomass of tree stand was approximated by the subsequent formula:

$$M_t = N \cdot \frac{m_l}{1000} + N \cdot \rho \cdot v, \quad (16)$$

where  $M_t$  is the total biomass of tree stand [tonne of fresh mass per hectare],  $N$  is the number of trees per hectare,  $m_l$  is the biomass of leaves of the mean model tree [kg],  $\rho$  is the spruce green wood density,  $0.75 [t m^{-3}]$  (Suliński, 1993, 2007) and  $v$  is the volume of trunk and branches of the mean model tree [ $m^3$ ]. The biomass of the stem layer was calculated by applying the following formulae:

$$M_s = N \cdot \rho \cdot H_s \cdot \frac{\pi}{4} \cdot \left( \frac{D_{0.5}}{100} \right)^2, \quad (17)$$

where  $M_s$  is the total biomass inside the stem layer [tonne of fresh mass per hectare],  $N$  is the number of trees per hectare,  $\rho$  is spruce green wood density,  $0.75 [t m^{-3}]$  (Suliński, 1993, 2007),  $H_s$  is the height of the stem layer [m] and  $D_{0.5}$  is the diameter of trunk at the stem mid-height [cm]:

$$D_{0.5} = \overline{DBH} - t_s \left( \frac{H_s}{2} - 1.3 \right), \quad (18)$$

where  $\overline{DBH}$  is the mean diameter at the breast height [cm],  $H_s$  is the height of a stem layer [m],  $t_s$  is the mean trunk taperness in a tree stand:

$$t_s = \frac{\overline{DBH}}{H}, \quad (19)$$

where  $\overline{DBH}$  is the mean diameter at the breast height [cm] and  $H$  is the mean height of a tree stand. The total biomass inside the canopy ( $M_c$  [tonne of fresh mass per hectare]) was calculated as the difference between the total biomass of a tree stand ( $M_t$ ) and the total biomass inside a stem layer ( $M_s$ ):

$$M_c = M_t - M_s. \quad (20)$$

### References

- Aubinet, M., Heinesch, B., Yernaux, M., 2003. Horizontal and vertical CO<sub>2</sub> advection in a sloping forest. *Bound. Layer Meteorol.* 108, 397–417.
- Baldocchi, D.D., Meyers, T.P., 1988. Turbulence structure in a deciduous forest. *Bound. Layer Meteorol.* 43, 345–364.
- Bergen, J.D., 1971. Vertical profiles of windspeed in a pine stand. *Forest Sci.* 17, 314–322.
- Bruchwald, A., 1995. *Dendrometria*. Wydawnictwo. SGGS, Warszawa.
- Currie, I.G., 2003. *Fundamental Mechanics of Fluids*, third ed. McGraw-Hill, New York.
- Czarnowski, M.S., 1978. *Zarys ekologii roślin lądowych*. PWN, Warszawa.
- Czuraj, M., Radwański, B., Strzemeski, S., 1966. *Tablice miąższości drzew stojących*. PWRiL, Warszawa.
- Denmead, O.T., Bradley, E.F., 1985. Flux-gradient relationships in a forest canopy. In: Hutchison, B.A., Hicks, B.B. (Eds.), *The Forest-Atmosphere Interaction*. D. Reidel Publishing, pp. 421–442.
- Fassnacht, K.S., Gower, S.T., Norman, J.M., McMurtrie, R.E., 1994. A comparison of optical and direct methods for estimating foliage surface area index in forests. *Agric. Forest Meteorol.* 71, 183–207.
- Finnigan, J.J., 1985. Turbulence transport in flexible plants canopies. In: Hutchison, B.A., Hicks, B.B. (Eds.), *The Forest-Atmosphere Interaction*. D. Reidel Publishing, pp. 443–480.
- Fischenich, J.C., 1996. *Velocity and resistance in densely vegetated floodways*. Ph.D. Thesis, Colorado State University, 203 pp.
- Fons, R.G., 1940. Influence of forest cover on wind velocity. *J. Forest.* 38, 481–486.
- Giertych, M., 1996. Genetyczna wartość świerka istebniańskiego. *Sylwan* CXL 3, 29–38.
- Green, S.R., Grace, J., Hutchings, N.J., 1995. Observations of turbulent air flow in three stands of widely spaced Sitka spruce. *Agric. Forest Meteorol.* 74, 205–225.
- Inoue, E., 1963. On the turbulent structure of air flow within crop canopies. *J. Meteorol. Soc. Jpn.* 41, 317–326.
- Janson, L., 1996. Ocena jakości hodowlanej zasobów genowych najlepszych pochodzeń świerka w Polsce. *Sylwan* CXL 3, 47–54.
- Jonckheere, I., Muys, B., Coppin, P., 2005. Allometry and evaluation of in situ optical LAI determination in Scots pine: a case study in Belgium. *Tree Physiol.* 25, 723–732.
- Karmanova, I.V., Sudnitsyna, T.N., Ilina, N.A., 1987. *Prostranstviennaya struktura slozhnykh sosniakov*. Nauka, Moskva.

- Lalic, B., Mihailovic, D.T., 2002. A new approach in parameterization of momentum transport inside and above forest canopy under neutral conditions. Integrated assessment and decision support. In: Proc. First Biennial Meeting of the Int. Environmental Modelling and Software Society, vol. 2. IEMSS, Lugano, Switzerland, pp. 139–154.
- Lalic, B., Mihailovic, D.T., Rajkovic, B., Arsenic, I.D., Radlovic, D., 2003. Wind profile within the forest canopy and in the transition layer above it. *Environ. Model. Software* 18, 943–950.
- Landsberg, J.J., James, G.B., 1971. Wind profiles in plant canopies: studies on an analytical model. *J. Appl. Ecol.* 8, 729–741.
- Lee, X., 2000. Air motion within and above forest vegetation in non-ideal conditions. *Forest Ecol. Manage.* 135, 3–18.
- Lemon, E., Allen, L.H., Muller, L., 1970. Carbon dioxide exchange of a tropical rain forest. *J. BioScience* 20, 1054–1059.
- Lieseback, M., Rau, H.-M., König, A.O., 2010. Fichtenherkunftsversuch von 1962 und IUFRO-Fichtenherkunftsversuch von 1972. Universitätsverlag Göttingen.
- Małek, S., Gawęda, T., 2005. Historia lasów zlewni Potok Dupniański w Beskidzie Śląskim. *Sylvan* 9, 51–58.
- Marcolla, B., Cescatti, A., Montagnani, L., Manca, G., Kerschbaumer, G., Minerbi, S., 2005. Importance of advection in the atmospheric CO<sub>2</sub> exchanges of an alpine forest. *Agric. Forest Meteorol.* 130, 193–206.
- Massman, W., 1987. A comparative study of some mathematical models of the mean wind structure and aerodynamic drag of plant canopies. *Bound. Layer Meteorol.* 40, 179–197.
- Massman, W.J., 1997. An analytical one-dimensional model of momentum transfer by vegetation of arbitrary structure. *Bound. Layer Meteorol.* 83, 407–421.
- Massman, W.J., Weil, J.C., 1999. An analytical one-dimensional second-order closure of turbulence statistics and the lagrangian time scale within and above plant canopies of arbitrary structure. *Bound. Layer Meteorol.* 91, 81–107.
- McNaughton, K.G., 1989. Micrometeorology of shelter belts and forest edges. *Phil. Trans. R. Soc. Lond. B324*, 351–368.
- Meyers, T., Paw, U.K.T., 1986. Testing of a higher-order closure model for modeling airflow within and above plant canopies. *Bound. Layer Meteorol.* 37, 297–311.
- Oliver, H.R., 1971. Wind profiles in and above a forest canopy. *Quart. J. R. Meteorol. Soc.* 97, 548.
- Pacalaj, M., Longauer, R., Krajmerová, A., Gömöry, D., 2002. Effect of site altitude on the growth and survival of Norway spruce (*Picea abies* L.) provenances on the Slovak plots of IUFRO experiment 1972. *J. Forest Sci.* 48, 16–26.
- Peterson, D.L., Abrough, M.J., Landner, M.A., 1989. Leaf area of lodgepole pine and whitebark pine in a subalpine Sierra Nevada forest. *Can. J. Forest Res.* 19, 401–403.
- Prandtl, L., 1925. Über die ausgebildete turbulenz. *Z. Angew. Math. Mech.* 5, 136–139.
- Queck, R., Bernhofer, Ch., 2010. Constructing wind profiles in forests from limited measurements of wind and vegetation structure. *Agric. Forest Meteorol.* 150, 724–735.
- Raupach, M.R., Coppin, P.A., Legg, B.J., 1986. Experiments on scalar dispersion within a model plant canopy. Part I: the turbulence structure. *Bound. Layer Meteorol.* 35, 21–52.
- Raupach, M.R., Shaw, R.H., 1982. Averaging procedures for flow within vegetation canopies. *Bound. Layer Meteorol.* 22, 79–90.
- Schwappach, A., 1943. Ertragstafeln der wichtigeren Holzarten in tabellarischer und graphischer Form Merkur. Praha.
- Shaw, R.H., 1977. Secondary wind speed maxima inside plant canopies. *J. Appl. Meteorol.* 16, 514–521.
- Shinn, J.H., 1971. Steady-state two-dimensional air flow in forests and the disturbance of surface layer flow by a forest wall. Technical Report ECOM-5383, Atmospheric Sciences Laboratory, White Sands Missile Range, New Mexico, USA, 60pp.
- Slater, L.J., 1972. Cofluent hypergeometric functions. In: Abramowitz, M., Stegun, I.A. (Eds.), *Handbook of Mathematical Functions with Formulas, Graphs, and Mathematical Tables*. Dover, New York.
- Staebler, R.M., Fitzjarrald, D.R., 2004. Observing subcanopy CO<sub>2</sub> advection. *Agric. Forest Meteorol.* 122, 139–156.
- Suliński, J., 1993. Modelowanie bilansu wodnego w wymianie między atmosferą, drzewostanem i gruntem przy użyciu kryteriów ekologicznych. *Zeszyty Naukowe AR, Kraków, rozpr.* 179.
- Suliński, J., 1997. The Amount of biomass as a function of the height and density of a tree stand. In: *Proceeding of the Third National Conference on Application of Mathematics in Biology and Medicine, Mądralin*, pp. 85–90.
- Suliński, J., 2007. The tree-stand height and age based method for calculation of annual biomass production in a forest community. *Acta Agr. Silv. Ser. Silv.* 45, 89–119.
- Suliński, J., Starzak, R., 2009. Premises for the construction of balance equations of water losses in mountain forest soils. *J. Water Land Dev.* 13a, 329–345.
- Suliński, J., Sypka, P., 2000. Trial of identification of a solar radiation transmission formula within spruce tree stands. In: *Proceedings of the Sixth Conference on Application of Mathematics in Biology and Medicine, Zawoja*, pp. 132–137.
- Sypka, P., 2003. Analysis of daily periodic temperature variation of covering layer of Soil below Istebna Spruce Stand. In: *Proceedings of the Ninth Conference on Application of Mathematics in Biology and Medicine, Piwniczna*, pp. 80–85.
- Turner, D.P., Acker, S.A., Means, J.E., Garman, S.L., 2000. Assessing alternative allometric algorithms for estimating leaf area of Douglas-fir trees and stands. *Forest Ecol. Manage.* 126, 61–76.
- Turnipseed, A.A., Anderson, D.E., Blanken, P.D., Baugh, W.M., Monson, R.K., 2003. Airflows and turbulent flux measurements in mountainous terrain. Part 1: canopy and local effects. *Agric. Forest Meteorol.* 119, 1–21.
- von Kármán, T., 1930. Mechanische Ähnlichkeit und yurbulenz. *Nachr. Ges. Wiss. Göttingen Math. Phys. Kl.* 68, 58–76.
- Wilhelm, W.W., Ruwe, K., Schlemmer, M.R., 2000. Comparisons of three Leaf Area Index Meters in a Corn Canopy. *Crop Sci.* 40, 1179–1183.
- Wilson, N.R., Shaw, R.H., 1977. Higher-order closure model for canopy flow. *J. Appl. Meteorol.* 16, 1197–1205.
- Yi, C., Monson, R.K., Zhai, Z., Anderson, D.E., Lamb, B., Allwine, G., Turnipseed, A.A., Burns, S.P., 2005. Modelling and measuring the nocturnal drainage flow in a high-elevation, subalpine forest with complex terrain. *J. Geophys. Res.* 110, D22303, <http://dx.doi.org/10.1029/2005JD006282>.
- Yi, C., 2008. Momentum transfer within canopies. *J. Appl. Meteorol. Climatol.* 47, 262–275.
- Zeng, P., Takahashi, H., 2000. A first-order closure model for the wind flow within and above vegetation canopies. *Agric. Forest Meteorol.* 103, 301–313.
- Zhu, J., Matsuzaki, T., Sakioka, K., 2000. Wind speeds within a single crown of Japanese black pine (*Pinus thunbergii* Parl.). *Agric. Forest Meteorol.* 135, 19–31.